

Thermo-Inductive Surface Crack Detection in Metallic Materials

Beate OSWALD-TRANTA, Gernot WALLY,
Institute for Automation, University of Leoben, Austria

Abstract. In the case of thermo-inductive testing the material is heated by induced eddy currents and the emission from the material surface is detected by an infrared camera. Anomalies in the surface temperature correspond to in-homogeneities in the material. The penetration depth of the induced eddy current depends on the induction-frequency and on the material properties as e.g. on the relative permeability value. In the case of magnetic materials, like steel, and a high excitation frequency, the penetration depth of the current is very small. Therefore, the eddy current 'flows around' surface cracks with a depth of 0.1-1mm. In contrast, in stainless steel the eddy current at the same excitation frequency has a much larger penetration depth and therefore leads to a different behaviour around a crack of similar depth and one observes lower temperatures around the crack. Finite element simulations have been carried out, in order to model the temperature distribution caused by the eddy currents. It is shown, that depending on the material properties, on the excitation frequency and on the duration of the heating pulse one gets higher or lower temperatures around the surface crack. The results of the simulations are compared with the experimental results.

Introduction

Thermo-inductive probing [1,2,3,4,5,6,7] is a thermo-graphic non-destructive testing method to detect shallow surface cracks in metallic materials. The technique uses induced eddy current to heat the material being tested. The heat dissipation due to the eddy current and the resistance of the material causes local heating. The infrared emission from the material surface is detected by a suitable imaging system. Anomalies in the surface heating correspond to in-homogeneities in the material. The technique can be used for the inspection and detection of macroscopic cracks in materials where eddy currents can be induced, whereby metals are particularly well suited.

In experiments it has been observed, that in the case of magnetic materials the surface cracks can be detected by an additional temperature increase around the cracks. It has been shown [7] that the deeper the surface crack is, the higher is the temperature increase at the edges of the crack. A formula has been derived [7,8], which allows the crack-depth to be determined from the measured temperature increase.

In the case of non-magnetic materials experiments show that a lower temperature occurs at the edges of the cracks and high temperatures at the tip of the crack [5,6]. The goal of this paper is to model the eddy current distribution inside the material and calculate the temperature distribution around long surface cracks for different parameters. It is investigated, under which circumstances one gets lower and higher temperature values at the edges of surface crack and how this information can be used to optimise the thermo-inductive probing for detection of surface cracks.

1. Experimental results

Thermo-inductive measurements have been carried out on different workpieces. The experimental setup is shown in Figure 1, whereas the tested magnetic steel is inserted into an induction coil. There are two surface cracks with a depth of about 1-3mm along the piece. The infrared camera is looking at the heated steel probe through the free space of the coil windings.

The camera is triggered externally to record a thermal image after a very short heating period. Figure 2 shows the infrared image after 0.1 sec heating. The surface cracks and the corners of the workpiece are additionally warmer than the steel sample itself.

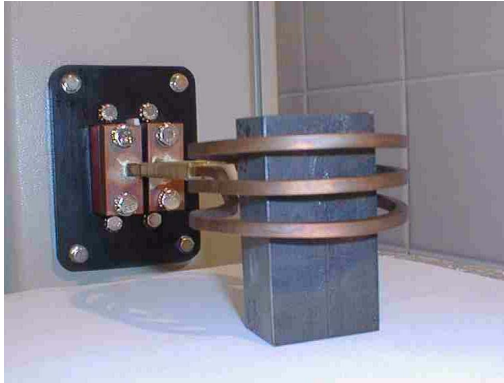


Figure 1: Inductive heating of a steel workpiece inserted into the induction coil.

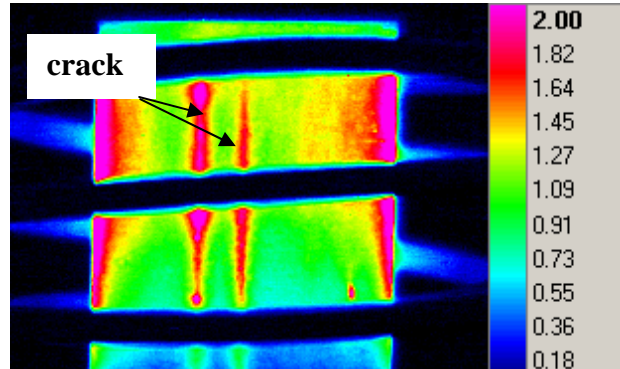


Figure 2: Infrared image of the heated steel shown in Figure 1.

Figure 3 shows the infrared image of an inductive heated stainless steel wire. The shallow surface crack along the wire can be seen very well by the temperature decrease around it. These experiments demonstrate that in magnetic materials the crack is visible by higher temperatures and in non-magnetic materials by lower temperatures.

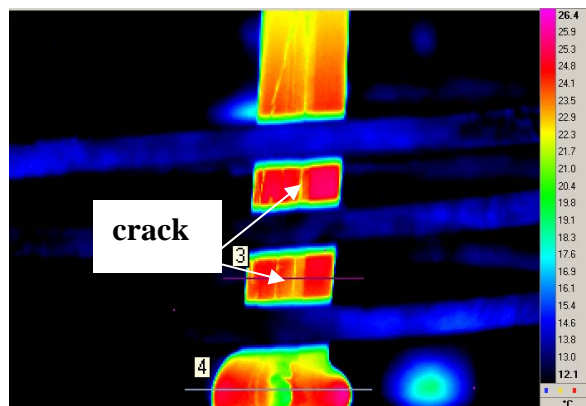


Figure 3: Infrared image of the heated stainless steel wire.

Further experiments have been carried out on sheet plates of steel with low magnetic permeability. The plate has been placed in the middle of an induction coil. Figure 4 and 5 show infrared images after a short heating period. In Figure 4 one can see that the corners of the steel square plate are colder than the sides of the workpiece. Figure 5 shows a workpiece of a long rectangle where a notch with a depth of 2 mm has been cut into the sheet. The tip of the notch is visible by a small circle of high temperature region, but the corners of this crack are colder than the sides of the rectangle. In the case of thermo-

inductive testing of long pieces as shown in Figure 3, we don't see the tip of the surface crack, which is hidden, but only the temperature on the surface that means the colder temperature on the edge of the crack.

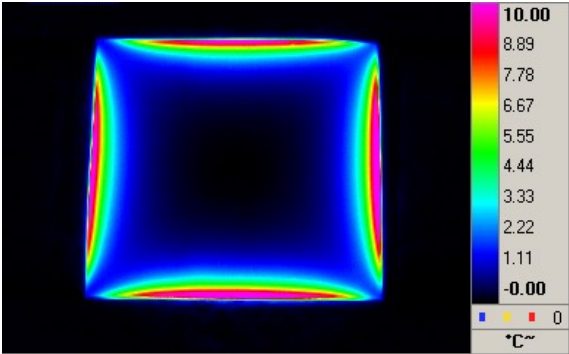


Figure 4: Infrared image of the heated steel sheet which forms a square

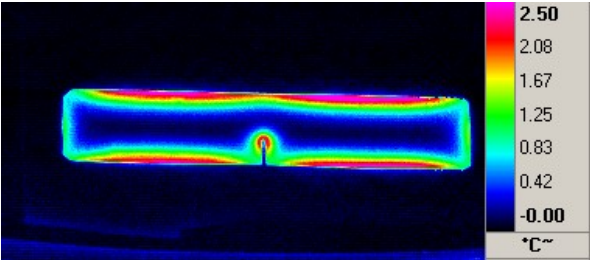


Figure 5: Infrared image of the heated steel sheet with an artificial crack

2. Calculations for a rectangle workpiece

In the first step the temperature distribution in an inductively heated long material with a square cross-section is investigated. In the next chapter the temperature distribution around a surface crack will be calculated for different cases.

It is well-known, that the induced eddy current decays exponentially below the surface, therefore it penetrates only a thin skin (so-called skin-effect). The coefficient of this exponential function depends mainly on the magnetic permeability value of the material and on the excitation frequency. The exponential function is strictly valid only for a semi-infinite long plain metal surface [9]. For other geometries the distribution of the eddy current can be numerically calculated. Figures 6 and 7 show isolines of the magnetic field in one corner of a square material. The lines have been calculated by the finite element simulator ANSYS [10]. Using the Maxwell-equations one can show, that in the case of a very long workpiece these lines are identical with the streamlines of the eddy current. Figure 6 shows the streamlines in a 7x7mm area at the corner for the case of a penetration depth of 1 mm. Figure 7 depicts a smaller area of 2x2 mm around the corner for the case that the penetration depth is only 0.1mm. One can see, that far away from the corner the eddy current is flowing parallel to the surface, but at the corner the current is pushed more inside the material, therefore it flows in a larger distance from the surface.

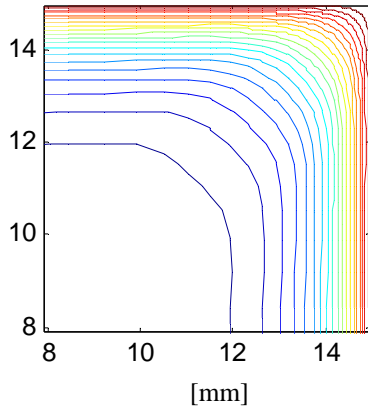


Figure 6: Calculated streamlines in the corner of a workpiece (penetration depth of the eddy current is 1mm)

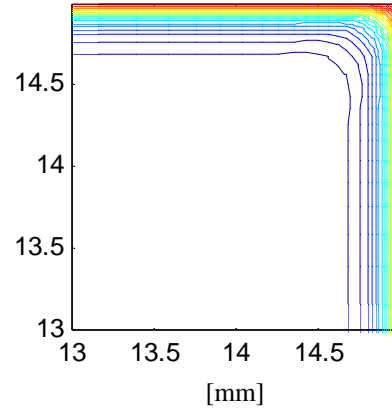


Figure 7: Calculated streamlines in the corner of a workpiece (penetration depth of the eddy current is 0.1mm)

The induced eddy current generates heat in the material due to its electrical resistance. The produced heat flows immediately inside the material. Because the density of the eddy current is less in the corner and the current is flowing farer away from the corner (see Figure 6), after a short heating period the corner of the square is colder than its sides. Figure 8 shows the temperature distribution after a heating period of 0.01 sec in the case, that the penetration depth is 1mm. This temperature distribution has been calculated by the ANSYS multi-physics finite element simulation package coupling the electrical and thermal phenomena. Due to the high heat conductivity of the metal, the generated heat spreads out very quickly. In the corner of the square occurs a heat accumulation, and therefore after a longer heating period the corner becomes warmer than the sides of the square, see Figure 9.

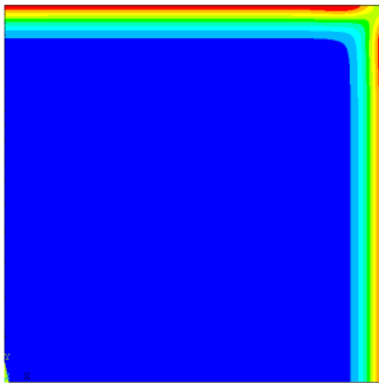


Figure 8: Calculated temperature distribution in one corner of a square after 0.01sec inductive heating, the penetration depth of the eddy current is 1mm. The size of the shown area is 15x15mm.

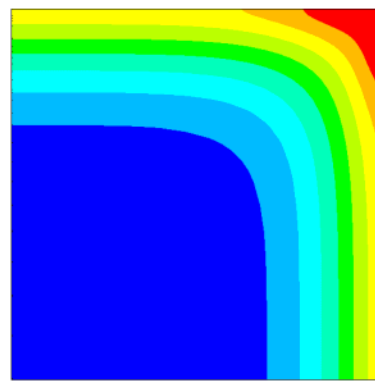


Figure 9: Calculated temperature distribution for the same case as shown in Figure 8, but after a heating period of 0.4 sec.

The smaller the penetration depth of the eddy current, the shorter is the first phase of the heating, when a colder corner can be observed. For the case of a penetration depth of 0.1mm, as depicted in Figure 7, the first phase is very short and already after 0.01 sec heating period the heat is accumulated in the corner and the corner is warmer, see Figure 10.

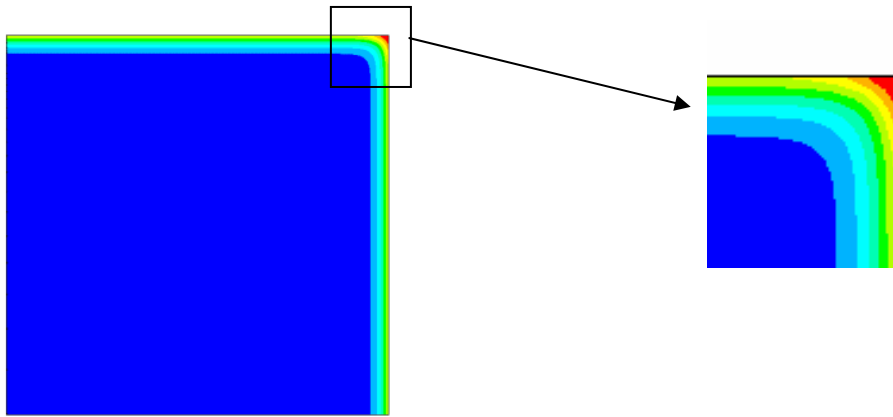


Figure 10: Calculated temperature distribution in a corner of a square after 0.01sec inductive heating, with a penetration depth of the eddy current of 0.1mm. The size of the shown area is 15x15mm. At the right side of the figure the temperature distribution in the corner is shown enlarged.

In order to compare the temperature distribution for different values of the penetration depth, Figure 11 shows the ratio between the temperature increase in the corner (ΔT_c) and the temperature increase at the side of the probe (ΔT_s) versus the heating period. In the case of larger penetration depth ($>0.7\text{mm}$) and short heating period the ratio is less than 1, which means, that the corner is colder than the side (this case is depicted in Figure 8). For longer heating periods the ratio becomes larger than 1 and the corner becomes warmer (as shown in Figure 9). If the penetration depth is very small, then the ratio becomes almost immediately larger than 1 (see also Figure 10) and approaches to 2. When the penetration depth is negligible small, then the temperature increase in the corner is twice of the temperature increase at the side of the square [7].

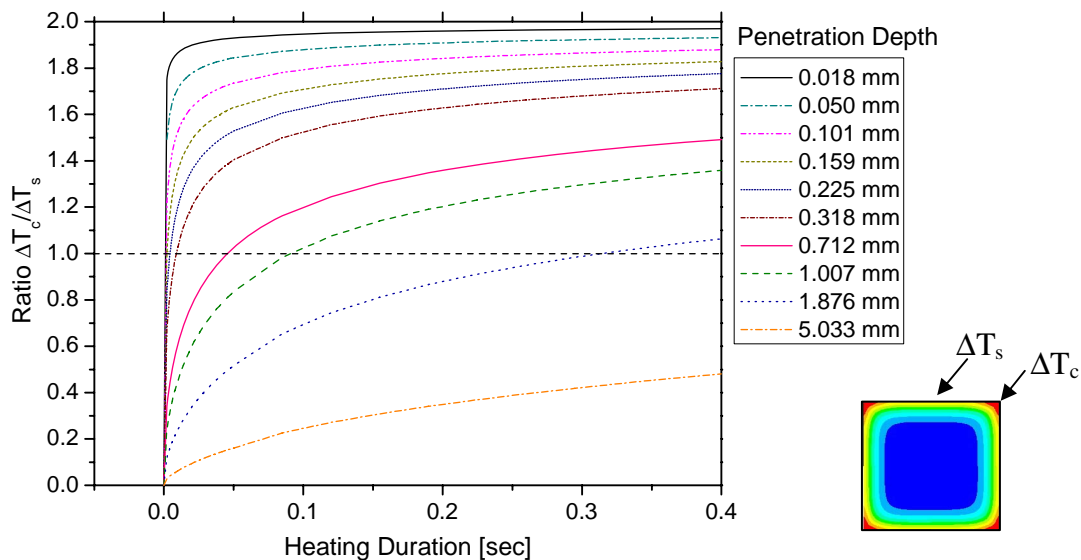


Figure 11: Ratio between the temperature increase in the corner and at the side of the square as a function of the heating period for different penetration depth values. The insert shows the definition of the temperatures.

3. Calculations for a surface crack

If there is a crack in the surface, then the induced eddy current is flowing around it. For a surface crack with a depth of 1 mm the calculated streamlines are depicted in Figure 12 and 13 for a penetration depth of 1 mm and for 0.1mm, respectively. If the penetration depth of the eddy current is comparable with the depth of the crack (see Figure 12), then the current is pushed from the edges of the crack inside the material, causing a lower current density at the edges of the crack but resulting in a higher current density around the tip of the crack. Therefore, after a very short heating period the tip of the crack is warmer, but the edge of the crack is colder than the surface of material, see Figure 14. After a longer heating period the heat is more or less homogenously distributed along the side of the crack, see Figure 15 and no heat accumulation can be observed in the corner of the crack.

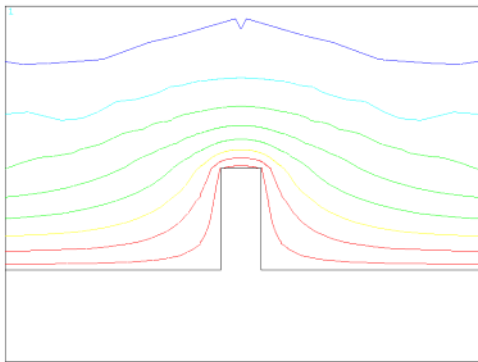


Figure 12: Calculated streamlines around a surface crack with a depth of 1mm (penetration depth of the eddy current is 1mm)

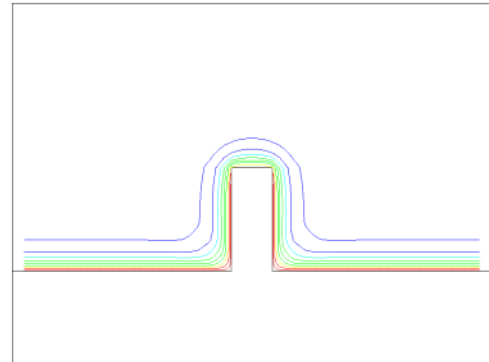


Figure 13: Calculated streamlines around a surface crack with a depth of 1mm (penetration depth of the eddy current is 0.1mm)

If the penetration depth of the eddy current is significantly smaller than surface crack, then the current is following more or less along the side of the crack, see in Figure 13. Therefore, the edge of the crack becomes warmer already after very short heating duration, see Figure 16.

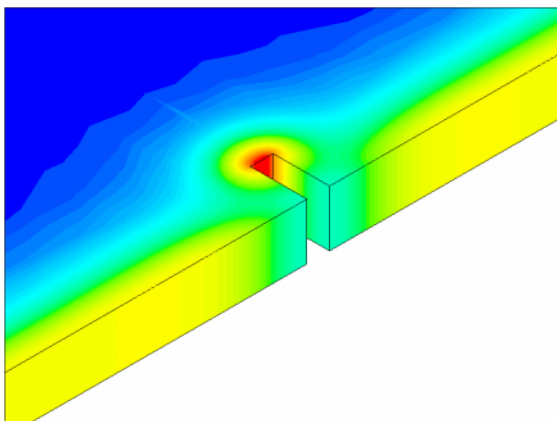


Figure 14: Calculated temperature distribution around a surface crack with a depth of 1mm after 0.01sec inductive heating. The penetration depth of the eddy current is 1mm.

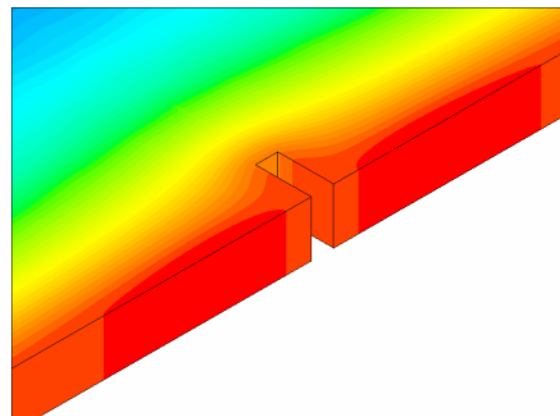


Figure 15: Calculated temperature distribution for the same case as shown in Figure 14, but after a heating period of 0.4 sec.

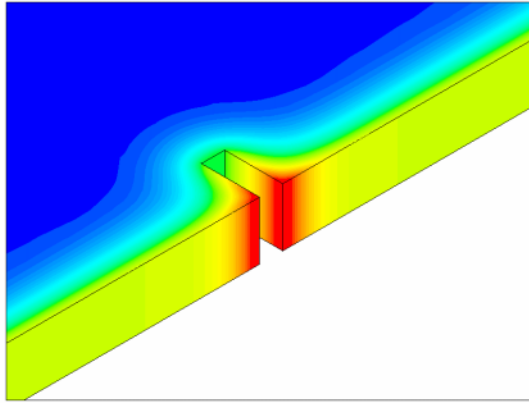


Figure 16: Calculated temperature distribution around a surface crack with a depth of 1mm after 0.01sec inductive heating. The penetration depth of the eddy current is 0.1mm.

Figure 17 shows the ratio between the temperature increase at the edge of the crack (ΔT_c) and the temperature increase at the side of the sample (ΔT_s) versus the heating period. If the penetration depth is 1mm, then the ratio is increasing with the heating duration, but it remains less than 1. This means, that the corner of the crack is at beginning colder than the side, but after a time the temperature becomes more or less uniform at the surface. These results are in very good agreement with the experimental results, shown in Figure 3.

In the case of smaller penetration depth, as the second curve shows in Figure 17 for a value of 0.159mm, after a short heating period the corner of the crack is warmer than the side, therefore the ratio is larger than 1. With increasing heating time the ratio becomes smaller, that means, the additional temperature increase around the crack becomes less. These simulation results are in very good agreement with the experimental results, shown in Figure 2.

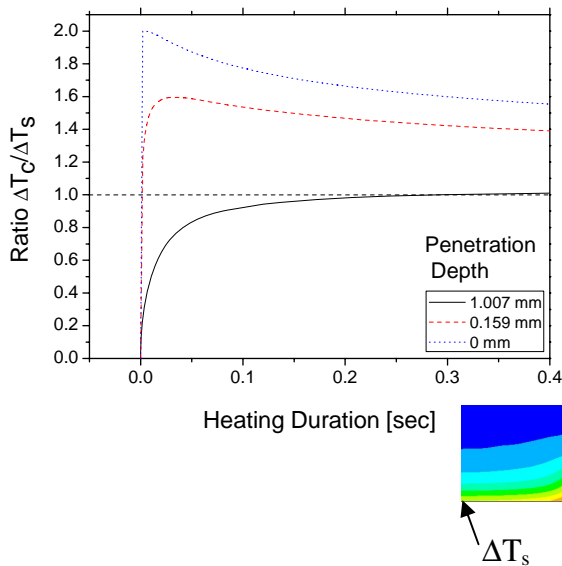


Figure 17: Ratio between the temperature increase in the corner of the crack and at the side of the sample as a function of the heating period for different penetration depth values. The insert shows the definition of the temperatures.

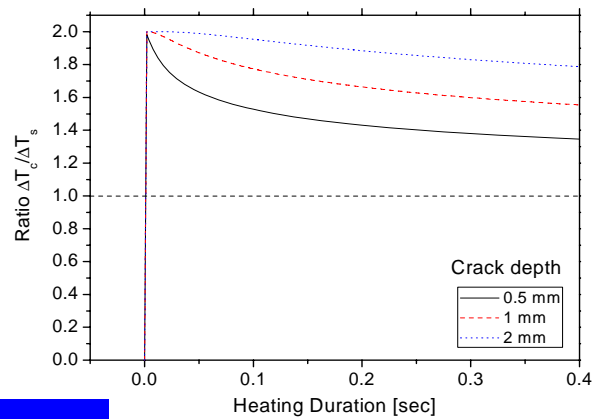


Figure 18: Ratio between the temperature increase in the corner of the crack and at the side of the sample as a function of the heating period for different crack depth values. The curves are calculated with the analytical model of [7,8].

If the penetration depth is negligible small, then the model can be calculated with the simplification, that the heat is applied only at the surface of the sample. For this case the equations, describing the temperature distribution around a surface crack, have been derived in [7] and [8]. Using these equations the third curve in Figure 17 has been calculated for the theoretical limit of a zero penetration depth. The curve shows, that immediately after switching on the inductive heating, the temperature ratio is 2 and with increasing time it becomes less and less.

Figure 18 shows the temperature ratio for different crack depth values, calculated by the analytical model [7,8] applying the heat on the surface of the sample. One can see from the curves, that the smaller is the crack, the earlier diminishes the additional heating around the crack, because a smaller crack is earlier overcome by the diffusion of the heat.

4. Summary

Experimental and simulation results have been shown, consistently demonstrating that surface cracks can be identified with the thermo-inductive technique. After a short heating period in magnetic materials cracks are made visible by higher temperatures and in non-magnetic materials by lower temperatures.

References

- [1] Nipponn Steel Corp., “Method of detecting a surface flaw of metallic material”, Patent No US4109508, 1978.
- [2] Elkem, “Detection of flaws in metal members”, Patent No Re32166, 1979.
- [3] Elkem, “Method of flaw detection in billets”, Patent No US4480928, 1984.
- [4] G.Busse, “Verfahren zur phasenempfindlichen Darstellung eines effektmodulierten Gegenstandes“, Patent No DE4203272, 1992.
- [5] T.Sakagami,S.Kubo, “Development of a new crack identification method based on singular current field using differential thermography”, Proceedings of SPIE 3700 369-376, 1999.
- [6] J.Bamberg, G.Erbeck, G.Zenzinger, „EddyTherm: Ein Verfahren zur bildgebenden Rißprüfung metallischer Bauteile“ ZfP-Zeitung 68, p.60 – 62, 1999.
- [7] B. Oswald-Tranta, “Thermoinductive Investigations of Magnetic Materials for Surface Cracks“, QIRT Journal Vol.1., p.33-46. 2004
- [8] B. Oswald-Tranta, G.Wally, “Thermo-inductive investigations of steel wires for surface cracks”, ThermoSense XXVII, Orlando, Proceedings of SPIE Vol. 5782, p.245-254
- [9] K.Simonyi, “Theoretische Elektrotechnik”, Barth Verlagsgesellschaft mbH, 1993.
- [10] <http://www.ansys.com>